SUPPORTING INFORMATION

Oxytocin enhances the pain-relieving effects of social support in romantic couples

Ann-Kathrin Kreuder, Lea Wassermann, Michael Wollseifer, Beate Ditzen, Monika Eckstein, Birgit Stoffel-Wagner, Juergen Hennig, René Hurlemann and Dirk Scheele

Supplementary Methods

Subjects

All subjects were in a romantic relationship for more than five months. The duration of the romantic relationships was comparable between the oxytocin (OXT) group (35.45 ± 24.96 months) and the placebo (PLC) group (34.19 ± 23.87 months; $t_{(94)} = -0.25$, $P = 0.80$, $d = -0.05$). In a screening session prior to the testing sessions, we assessed social anxiety using a German version (Stangier et al., 1999) of the Social Interaction Anxiety Scale and the Social Phobia Scale (Mattick and Clarke, 1998) and depressive symptoms with the Beck Depression Inventory (Hautzinger et al., 1995). Autistic-like traits were measured via the Autism Spectrum Quotient questionnaire (Baron-Cohen et al., 2001). The "EROS" subscale for romantic love of the Marburg Attitude Inventory of Love Styles (Bierhoff et al., 1993) was used to measure the subjects' relationship quality. Treatment groups did not differ in the abovementioned questionnaire data (all *P*s > 0.19; cf. **Supplementary Table S5**). All subjects were naive to prescription-strength psychoactive medication. Contraindications for MRI scanning were additional exclusion criteria. For female participants, the use of hormonal contraceptives, birth of a child and pregnancy were additional exclusion criteria. In a personal interview on the testing day, the subjects were asked if anything of personal significance had changed in their romantic relationships (e.g., moving in together). Only one couple mentioned that they had a dispute two days before the MRI session.

The participants were asked to maintain their regular sleeping and waking times and to abstain from caffeine and alcohol intake on the day of the experiment. To control for potentially confounding effects of OXT on state anxiety and mood, all subjects completed the State-Trait Anxiety Inventory (STAI) (Spielberger et al., 1970) and the Positive and Negative Affective Scale (PANAS) (Watson et al., 1998) immediately before the administration of the treatment and after the experiment. Three mixed analyses of variance (ANOVA) with the time point (before the experiment, after the experiment) as a within-subjects factor, treatment (OXT, PLC) as a between-

subjects factor, and state anxiety, positive affect, or negative affect as dependent variable revealed no significant main effect of treatment or an interaction between treatment and time point (all *P*s > 0.25; cf. **Supplementary Table S3**). Thus, OXT did not influence subjective anxiety or mood ratings. After completing the task, subjects were asked to guess whether they had received OXT or PLC. The estimation of the received treatment was comparable between the OXT and PLC group ($\chi^2_{(1)} = 0.34$, $P = 0.56$, $W = 0.06$), showing that the subjects were unaware of whether they had received OXT or PLC. Five subjects in the PLC group and three subjects in the OXT group reported side effects (headache, slight dizziness, fatigue, and cold feet). Finally, the subjects were asked after the experimental paradigm whether they had any doubts regarding the task-dependent cover story. None of the participants mentioned any doubts. To determine baseline OXT levels in the PLC and OXT group, one saliva sample from each subject was collected before the administration of the nasal spray (cf. **Supplementary Table S4**).

Electric Stimulation and Determining Pain Thresholds

The electric stimulation consisted of brief electric shocks of 4 msec duration. The electric stimuli were delivered via a Biopac stimulator module STM100C and a STIMSOC adapter (Biopac Systems, Inc., Goleta CA, USA) coupled with the notebook computer presenting the fMRI paradigm. The current was passed from the generator to the subject via two MRI-compatible Ag/AgCl electrodes filled with electrolyte gel on the subject's left (non-dominant) dorsal lower arm. In a screening session prior to the fMRI acquisition day, the subjects' individual shock intensity levels were set by applying gradually more intense shocks until the subject reported the shock was "highly annoying yet not painful".

Functional MRI Paradigm

Using Presentation 14 (Neurobehavioral Systems, Albany, CA), stimuli were presented on a 32-inch MRI compatible TFT LCD monitor (NordicNeuroLab, Bergen, Norway) placed at the rear

of the magnet bore. In the screening session, standardized photographs were made of all participants, who were asked to wear a white t-shirt and dark pants. The brightness and size of the pictures were kept constant. Before the social support fMRI task, the subjects underwent another unrelated fMRI paradigm. The results regarding this paradigm are reported elsewhere (Kreuder et al., 2017). The order of the two fMRI paradigms was fixed across the whole study.

Acquisition of fMRI Data

A Siemens Trio MRI system (Siemens, Erlangen, Germany) operating at 3T and a 32 channel head coil were used to obtain T2*-weighted echoplanar (EPI) images with blood-oxygen-level-dependent contrast (TR = 2500 ms, TE = 30 ms, matrix size: 96 x 96, pixel size: 2 x 2 mm, slice thickness = 3.0 mm, distance factor = 10%, flip angle = 90°, 37 transversal slices). In addition, high-resolution anatomical images were acquired on the same scanner using a T1-weighted 3D MPRAGE sequence (imaging parameters: TR = 1660 ms, TE = 2.54 ms, matrix size: 320 x 320, pixel size: 0.8 x 0.8 mm, slice thickness = 0.79 mm, flip angle = 9°, 208 sagittal slices).

Analysis of fMRI Data

Functional MRI data were preprocessed and analyzed using SPM12 software (Wellcome Trust Center for Neuroimaging, London, UK; http://www.fil.ion.ucl.ac.uk/spm) implemented in Matlab (The MathWorks Inc., Natick, MA). The first five volumes of each functional time series were discarded to allow for T1 equilibration. Images were corrected for head movement between scans by an affine registration. For realignment, a two-pass procedure was used by which images were initially realigned to the first image of the time series and subsequently re-realigned to the mean of all images.

For normalization, a two-step procedure was applied. Normalization parameters were first determined using the co-registered individual T1 image as the source and the multi subject T1-template integrated in SPM12. This step included by default tissue segmentation using tissue

probability maps. Next, normalization parameters were applied to normalize the functional images. Finally, these images were presented in standard anatomical Montreal Neurological Institute (MNI) space and resampled at 2 x 2 x 2 mm^3 voxel size. The normalized images were spatially smoothed using a 6-mm FWHM Gaussian kernel. Raw time series were detrended by the application of a high-pass filter (cut-off period, 128 sec). On the second level, a 2 x 3 flexible factorial design with treatment (OXT, PLC) as a between-subject factor, type of support (partner, stranger, no support) as a within-subject factor, and the BOLD-response of the contrasts [$Partner_{Shock>No\ Shock}$], [$Stranger_{Shock>No\ Shock}$], [No $Support_{Shock>No\ Shock}$] as dependent variables was conducted. Unspecific, domain-general effects of OXT (i.e., the main effect of treatment) were analyzed by comparing all conditions with the low level baseline ([OXT > PLC] and [OXT < PLC]). Sex-differential OXT effects on the processing of shocks versus no shocks under the different support conditions were analyzed by using a 2 x 2 flexible factorial design with treatment (OXT, PLC) and sex (male, female) as between-subject factors and the BOLD-response of the contrasts [$Partner_{Shock>No\ Shock}$ > $Stranger_{Shock>No\ Shock}$], [$Partner_{Shock>No\ Shock}$ > No $Support_{Shock>No\ Shock}$], and [$Stranger_{Shock>No\ Shock}$ > No $Support_{Shock>No\ Shock}$] as dependent variables. To further address OXT effects on the interplay of pain and social support-related brain regions, a generalized psychophysiological interactions (PPIs) analysis was conducted (McLaren et al., 2012). Based on the results of the BOLD analysis, we examined the modulation effects of OXT on functional connectivity between the middle prefrontal cortex and the anterior insula. For the bilateral middle prefrontal cortex as seed regions, we used spheres with a 6 mm radius centered at the maximum t-value of the BOLD treatment effect (MNI coordinates x, y, z = ± 36, 18, 50). The bilateral anterior insula as seed regions were defined by applying a caudal boundary of y = 8 to the structural defined insula implemented in the WFU Pick atlas. In a first step of the gPPI analysis, the volume (number of voxels) of the seed region was estimated. The gPPI analysis can only be calculated for subjects who did not have volume reduction in the seed region. After assessing the quality of the neural data, we excluded participants with a reduced number of voxels in one of the seed regions from the following

functional connectivity analyses. For the right AI as a seed region, nine subjects were excluded due to a reduced number of voxels in the seed region, and for the right MFG, two subjects were excluded. The brain figures of the gPPI results were created using the BrainNet Viewer toolbox implemented in Matlab (Xia et al., 2013).

Statistical Analysis

Demographic, neuropsychological, and behavioral data were tested using IBM SPSS Statistic 24 (IBM, New York, NY, USA). Quantitative behavioral data were compared by mixed ANOVA and dependent and independent t-tests. Pearson's product-moment correlation was used for correlation analysis. Eta-squared and Cohen's d were calculated as measures of effect size. For qualitative variables, Pearson's chi-squared tests were used. All reported *P*-values are two-tailed. *P*-values of $P < 0.05$ were considered significant and *P*-values of $P < 0.10$ as trend-to-significant.

Hormonal Assessment

Salivary OXT samples were collected using pre-chilled Salivettes (Sarstedt, Rommelsdorf, Germany). The OXT saliva sample was collected before administration of the nasal spray. Salivettes were immediately centrifuged at 4180 g for 3 min and aliquoted samples were stored at -80°C until assayed. Saliva OXT was extracted and quantified using a highly sensitive and specific radioimmunoassay (RIAgnosis, Munich, Germany). The limit of detection was 0.1 - 0.5 pg, depending on the age of the tracer. Intra-assay and inter-assay coefficients of variability were < 10%. All samples to be compared were assayed in the same batch, i.e., under intra-assay conditions.

Serum FSH, LH, and estradiol were analyzed by fully automated homogeneous sandwich chemiluminescent immunoassays based on the LOCI™ technology on a Dimension Vista™ system according to the manufacturer´s instructions (Siemens Healthcare Diagnostics, Marburg, Germany). The detection limits of each assay were 0.2 IU/l for LH and FSH and 11 pg/ml for

estradiol, respectively. The coefficients of variation for intra-assay and inter-assay precision were <1.8 % and <2.1 % for LH, <1.9 % and <2.2 % for FSH, and <5.5 % and <5.9 % for estradiol, respectively. Serum progesterone was determined by a fully automated solid-phase competitive chemiluminescent enzyme immunoassay on an Immulite™ 2000xpi system according to the manufacturer´s instructions (Siemens Healthcare Diagnostics). The detection limit of the assay was 0.1 ng/ml. The coefficients of variation for intra-assay and inter-assay precision were <4.2 % and <5.5 %. The cross-reactivity of all assays with other related compounds was minimal. Serum testosterone was determined by a competitive enzyme immunoassay (ELISA) according to the manufacturer´s instructions (IBL International, Hamburg, Germany). The detection limit of the assay was 4.7 pg/ml. The coefficients of variation for intra-assay and inter-assay precision were <7.1 % and <7.7 %.

Supplementary Results

Behavioral Results

We tested whether the anti-nociceptive effects of OXT and the effects of the different support conditions on the experience of shock and no shock events differed between subjects with higher and lower levels of romantic love, assessed by the "EROS" scale of the MEIL. For this purpose, the EROS score was median dichotomized (EROS higher: 8.35 ± 0.35; EROS lower: 6.84 ± 0.85). A mixed ANOVA with treatment (OXT, PLC) and EROS (higher, lower) as between-subject factors and support type (partner, stranger, no support) and stimulus (shock, no shock) as within-subject factors was performed. We found a significant main effect of support type ($F_{(2,186)} = 72.73$, $P < 0.01$, $\eta^2 = 0.44$), a significant main effect of stimulus ($F_{(1,93)} = 226.21$, $P < 0.01$, $\eta^2 = 0.71$), a trend-to-significant interaction between stimulus and treatment ($F_{(1,93)} = 3.85$, $P = 0.05$, $\eta^2 = 0.04$), a trend-to-significant interaction between stimulus and support type ($F_{(2,186)} = 2.76$, $P = 0.07$, $\eta^2 = 0.03$) and a significant interaction between EROS and support type ($F_{(2,186)} = 9.53$, $P < 0.01$, $\eta^2 = 0.09$). Post-hoc independent t-tests showed that subjects with a higher level of romantic love rated partner support as significantly more pleasant than did subjects with a lower level of romantic love ($t_{(95)} = 2.32$, $P < 0.05$, $d = 0.47$), but did not differ in the ratings of stranger support ($t_{(95)} = 0.37$, $P = 0.71$, $d = 0.08$) and no support ($t_{(95)} = -1.14$, $P = 0.26$, $d = -0.23$). There were no other significant main or interaction effects (all Ps > 0.13). Accordingly, the anti-nociceptive effects of OXT did not differ between higher and lower EROS scorers, but higher EROS scorers rated partner support as more pleasant than EROS lower scorers did.

Furthermore, we found no significant association between baseline salivary OXT levels and the levels of romantic love "EROS" ($P \geq 0.65$). Likewise, two sample t-test revealed no significant differences in the salivary OXT levels between subjects with higher and lower levels of romantic love ($t_{(94)} = 0.09$, $P = 0.93$, $d = 0.02$).

To further examine a potential effect of sex on the experience of shock and no shocks under the different support conditions, we performed an additional mixed ANOVA with support type (partner, stranger, no support) and stimulus (shock, no shock) as within-subject factors and sex (male, female) and treatment (OXT, PLC) as between-subject factors. We obtained a significant main effect of support type ($F_{(2,186)} = 53.77$, $P < 0.01$, $\eta^2 = 0.36$), a significant main effect of stimulus ($F_{(1,93)} = 210.68$, $P < 0.01$, $\eta^2 = 0.69$), and a trend-to-significant interaction between stimulus and treatment ($F_{(1,93)} = 3.74$, $P = 0.06$, $\eta^2 = 0.04$). Furthermore, the ANOVA yielded no significant main or interaction effects of sex (all *P*s > 0.12).

To explore possible effects of the relationship duration, we performed an additional correlation analysis between the duration of the subjects' romantic relationship (in months) and the behavioral responses to shocks and no shocks under partner support. This analysis showed no significant associations (PLC: all *P*s ≥ 0.19, OXT: all *P*s ≥ 0.28).

Finally, in the PLC group, we examined a possible correlation between the baseline salivary OXT levels and the unpleasantness ratings. This analysis yielded no significant correlations (all *Ps* ≥ 0.30).

fMRI Results and Functional Connectivity

Initially, we contrasted the neural activity to shocks versus no shocks under OXT and PLC. This analysis revealed no significant group differences in the neural activity to shocks relative to no shocks across support conditions on the whole brain level or in the *a priori* defined ROIs (all *P*s > 0.05).

As described in the fMRI results section of the main manuscript, OXT significantly augmented the beneficial effect of partner support relative to no support in the left AI (cf. **Figure 3A**). Furthermore, we found a trend-to-significant effect of OXT in enhancing the beneficial effect of partner support relative to stranger support in the left AI (i.e., diminished the response to shocks

versus no shocks in the AI under partner support compared to stranger support; -30, 24, -8; $t_{(270)}$ = 3.37, P_{FWE} = 0.07, d = 0.53).

As described in the behavioral results section of the main manuscript, we found a significant positive correlation between the subjects' level of romantic love and the support effect of the partner compared to no support on the experience of shocks in the OXT group (cf. **Figure 1C**). Hence, we examined whether the facilitating effect of OXT on the anti-nociceptive effects of partner support differed between subjects with higher and lower EROS. Using the neural activity to the contrast [$\text{Partner}_{\text{Shock>No Shock}}$ > $\text{No Support}_{\text{Shock>No Shock}}$] as the dependent variable in a flexible factorial design, we found no significant interaction between treatment and EROS and no significant main effect of EROS on the whole brain level or in the a priori defined ROIs (all *P*s > 0.05). However, using the neural response to the contrast [$\text{Partner}_{\text{Shock>No Shock}}$ > $\text{Stranger}_{\text{Shock>No Shock}}$] as the dependent variable in a flexible factorial design revealed a significant interaction between treatment and EROS in the left AI (-30, 20, 10; $t_{(88)}$ = 3.93, P_{FWE} < 0.05, d = 0.67). The OXT effect on partner support compared to stranger support (i.e., reduced response to shocks versus no shocks in the left AI under partner support compared to stranger support) was more pronounced in subjects with a higher level of romantic love.

Furthermore, adding the median-dichotomized variable OXT levels (low, high) as a between-subject factor to the flexible factorial design did not yield a significant interaction effect on the neural response to [$\text{Partner}_{\text{Shock>No Shock}}$ > $\text{No Support}_{\text{Shock>No Shock}}$], [$\text{Partner}_{\text{Shock>No Shock}}$ > $\text{Stranger}_{\text{Shock>No Shock}}$], and [$\text{Stranger}_{\text{Shock>No Shock}}$ > $\text{No Support}_{\text{Shock>No Shock}}$] on whole brain level or in any of our a priori defined ROIs (all *P*s > 0.05).

Finally, an additional functional connectivity analysis showed that the administration of intranasal OXT resulted in diminished functional connectivity from the left AI (seed region) to the left AMY during shock relative to no shock trials (**A;** peak MNI coordinates x, y, z: -26, -14, -6; $t_{(240)}$ = 3.16, P_{FWE} < 0.05, d = 0.58, display threshold P < 0.05 uncorrected; cf. **Supplementary Figure S2 A**). In the whole sample, a stronger functional coupling of AMY and AI correlated with

more unpleasant experience of shocks (r = 0.24, P < 0.05; cf. **Supplementary Figure S2 B**), indicating that the unspecific anti-nociceptive effects of OXT could be driven by neuromodulatory changes in the interplay of AMY and AI.

Supplementary Tables

Table S1. Activation table for GLM analysis under PLC (Shock vs. No Shock)

Region	Right/left	Cluster size (voxels)	t-score	MNI coordinates		
				x	y	z
PLC: Shock > No Shock						
Lingual gyrus	L	1734	10.02	-14	-72	-10
Calcarine fissure	L		8.41	-8	-80	4
Vermis			7.14	-2	-64	-10
Insula	R	4629	9.21	40	2	-4
Insula	R		9.19	40	4	-12
Inferior frontal operculum	R		7.79	56	14	0
Insula	L	2870	8.80	-38	-2	-6
Insula	L		7.32	-34	0	12
Rolandic operculum	L		6.61	-56	4	2
Middle frontal gyrus	R	628	6.37	46	46	8
Middle frontal gyrus	R		5.90	44	42	18
Middle cingulate cortex	R	601	6.08	2	26	30
Anterior cingulate cortex	L		4.68	0	32	20
Anterior cingulate cortex	L		4.49	-2	34	10
Superior frontal gyrus	R	229	4.74	16	-70	52
PLC: No Shock > Shock						
Calcarine fissure	L	609	9.35	-8	-94	12
Middle occipital gyrus	L		4.89	-38	-88	4
Middle occipital gyrus	L		3.91	-36	-88	18
Lingual gyrus	R	1241	9.15	14	-70	-2
Lingual gyrus	R		4.91	24	-50	-8
Cuneus	R		4.88	16	-80	34
Angular gyrus	R	1369	6.18	46	-48	26
Middle temporal gyrus	R		5.56	52	-54	16
Angular gyrus	R		4.79	58	-56	26
Inferior occipital gyrus	L	978	6.05	-36	-80	-10
Inferior occipital gyrus	L		5.45	-44	-58	-12

Middle temporal gyrus	L		5.28	-58	-40	0
Middle cingulate cortex	L	3450	5.57	-4	-42	42
Precentral gyrus	R		5.51	12	-32	70
Supplementary motor area	R		5.32	8	-24	54
Angular gyrus	L	1457	5.31	-48	-52	24
Angular gyrus	L		5.06	-50	-60	24
Middle occipital gyrus	L		4.71	-30	-82	40
Inferior frontal operculum	L	683	5.13	-32	6	30
Inferior frontal gyrus, triangularis	L		4.73	-38	18	30
Inferior frontal gyrus, triangularis	L		4.34	-54	20	24
Medial frontal gyrus, orbitale	L	321	4.93	-6	34	-14
Medial frontal gyrus, orbitale	L		4.14	6	36	-14
Medial frontal gyrus, orbitale	L		4.03	0	42	-12
Middle frontal gyrus	R	366	4.50	-26	20	46
Middle frontal gyrus	R		4.10	-30	34	44
Middle frontal gyrus	R		4.02	-26	26	54
Superior frontal gyrus	L	168	3.73	24	22	38
Superior frontal gyrus	L		3.58	28	32	52

Notes. For the whole-brain analysis, a height threshold of $P < 0.001$ was used. Abbreviations: PLC, placebo.

Table S2. Activation table for GLM analysis under OXT (Shock vs. No Shock)

Region	Right/left	Cluster size (voxels)	t-score	MNI coordinates		
				x	y	z
OXT: Shock > No Shock						
Insula	R	4645	10.26	40	2	-6
Rolandic operculum	R		8.69	58	10	0
Inferior frontal gyrus, orbitale	R		8.54	50	18	-8
Lingual gyrus	L	2404	9.86	-8	-76	-10
Lingual gyrus	L		7.78	-12	-78	2
Lingual gyrus	L		7.11	-4	-82	0
Insula	L	4081	9.57	-38	-2	-6
Superior temporal gyrus	L		7.37	-38	-12	-8
Gyrus supramarginalis	L		7.36	-62	-22	18
Middle frontal gyrus	R	389	5.33	48	46	6
Middle frontal gyrus	R		4.67	38	44	2
Middle frontal gyrus	R		4.26	46	42	16
Middle cingulate cortex	R	406	4.35	2	12	34
Anterior cingulate cortex	R		4.17	2	26	26
Anterior cingulate cortex	R		3.66	12	32	16
OXT: No Shock > Shock						
Superior occipital gyrus	L	248	7.13	-12	-94	16
Middle occipital gyrus	L		4.91	-30	-92	14
Middle occipital gyrus	L		4.59	-16	-94	26
Middle temporal gyrus	R	634	5.84	58	-58	18
Angular gyrus	R		5.35	54	-66	28
Supramarginal gyrus	R		4.46	48	-44	24
Precuneus	L	702	4.90	-4	-48	40
Postcentral gyrus	R		4.58	14	-36	68
Precuneus	R		4.47	8	-50	42
Middle temporal gyrus	L	298	4.86	-50	-52	20
Middle occipital gyrus	L		3.74	-42	-76	32
Middle temporal gyrus	L		3.60	-40	-58	20
Paracentral lobule	L	149	4.39	-10	-34	66
Precuneus	L		3.85	-10	-44	66

Medial frontal gyrus, orbitale	R	159	4.36	4	30	-14
Medial frontal gyrus, orbitale	R		3.87	6	42	-14
Medial frontal gyrus, orbitale	L		3.39	-6	26	-12
Precentral gyrus	R	177	3.81	32	-24	56
Precentral gyrus	R		3.51	34	-18	48
Precentral gyrus	R		3.23	22	-22	66

Notes. For the whole-brain analysis, a height threshold of $P < 0.001$ was used. Abbreviations: OXT, oxytocin.

Table S3. State measurement of anxiety and attention

	OXT group (n = 49) Mean (± SD)	PLC group (n = 48) Mean (± SD)	t	P
PANAS positive pre [a]	30.37 (± 5.20)	31.15 (± 5.68)	0.70	0.48
PANAS positive post [a]	28.76 (± 7.46)	28.02 (± 6.90)	-0.50	0.62
PANAS negative pre [a]	11.84 (± 1.97)	12.10 (± 2.68)	0.56	0.58
PANAS negative post [a]	11.27 (± 1.75)	11.83 (± 2.96)	1.15	0.25
STAI state pre [b]	32.81 (± 5.88)	34.15 (± 7.93)	0.93	0.35
STAI state post [b]	33.24 (± 5.50)	32.98 (± 6.95)	-0.50	0.62

Notes. Mood before and after the fMRI experiment was assessed using the [a] PANAS = Positive and Negative Affect Schedule. State anxiety before and after the experiment was assessed using the [b] STAI = State Trait Anxiety Inventory. Abbreviations: OXT, oxytocin; PLC, placebo.

Table S4. Baseline measurement of endocrine factors

	OXT group (n = 16) Mean (± SD)	PLC group (n = 16) Mean (± SD)	*t*	*P*
Females				
Baseline Oxytocin (pg/ml)	0.91 (± 0.72)	0.92 (± 0.75)	0.01	0.99
Estradiol (pg/ml)	143.54 (± 94.10)	106.83 (± 46.70)	-1.40	0.17
FSH (U/l)	6.34 (± 9.65)	3.79 (± 1.46)	-1.05	0.30
LH (U/l)	9.76 (± 10.25)	6.81 (± 3.45)	-1.09	0.28
Progesterone (ng/ml)	6.34 (± 5.21)	6.17 (± 5.45)	-0.09	0.93
Testosterone (pg/ml)	0.22 (± 0.05)	0.25 (± 0.10)	0.74	0.47

	OXT group (n = 33) Mean (± SD)	PLC group (n = 32) Mean (± SD)	*t*	*P*
Males				
Baseline Oxytocin (pg/ml)	1.15 (± 0.71)	1.24 (± 0.79)	0.52	0.61
Estradiol (pg/ml)	24.83 (± 16.55)	24.42 (± 9.71)	-0.12	0.90
FSH (U/l)	3.39 (± 2.10)	3.86 (± 2.31)	0.85	0.40
LH (U/l)	3.82 (± 2.15)	4.36 (± 1.64)	1.13	0.26
Progesterone (ng/ml)	3.07 (± 9.06)	3.38 (± 9.69)	0.13	0.90
Testosterone (pg/ml)	3.31 (± 1.44)	3.62 (± 1.60)	0.81	0.42

Notes. There were no significant differences in any measurements between the OXT and PLC sessions (all *P*s > 0.05).

Abbreviations: FSH, follicle-stimulating hormone; LH, luteinizing hormone; OXT, oxytocin; PLC, placebo.

Table S5. Demographics and psychometric questionnaire data

	OXT group (n = 49) Mean (± SD)	PLC group (n = 48) Mean (± SD)	*t*	*P*
Age (years)	25.76 (± 3.71)	24.79 (± 3.27)	-1.32	0.19
Education (years)	16.76 (± 2.97)	16.83 (± 2.72)	0.11	0.91
Romantic relationship length (months)	35.45 (± 24.96)	34.19 (± 23.87)	-0.25	0.80
AQ [a]	14.84 (± 5.77)	15.42 (± 5.21)	0.52	0.61
BDI [b]	2.31 (± 2.84)	2.04 (± 3.06)	-0.44	0.66
MEIL EROS [c]	7.47 (± 1.03)	7.71 (± 0.88)	1.17	0.25
SIAS [d]	13.00 (± 8.20)	13.27 (± 7.67)	1.67	0.87
SPS [e]	4.86 (± 3.92)	5.75 (± 4.87)	1.00	0.32
STAI trait [f]	31.71 (± 5.86)	31.65 (± 7.54)	-0.05	0.96

Notes. Autistic-like traits were assessed by the [a] AQ (Autism Spectrum Quotient) and depressive symptoms were assessed by the [b] BDI (Beck's Depression Scale, Version II). Relationship quality was measured by the [c] MEIL EROS (Marburg Attitude Inventory of Love Styles; subscale for romantic love) and the attitude towards social interactions was measured by the [d] SIAS (Social Interaction Scale) and [e] SPS (Social Phobia Scale). Trait anxiety symptoms were measured by the [f] STAI (State Trait Anxiety inventory). Abbreviations: OXT, oxytocin; PLC, placebo.

Supplementary Figures

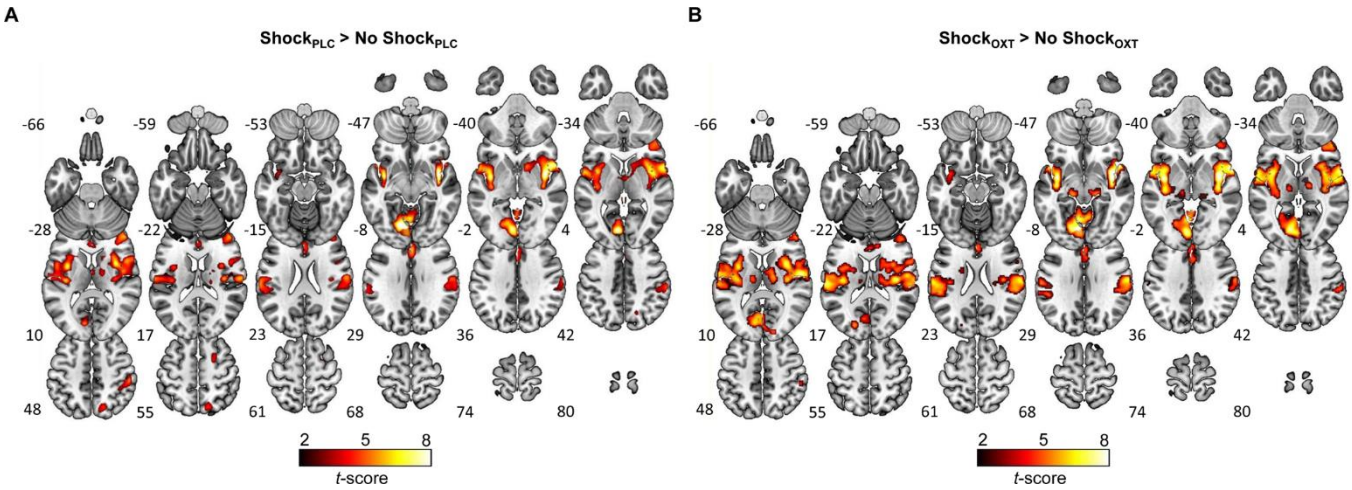

Figure S1. Whole-brain activation maps for the contrasts [Shock > No Shock] under placebo (**A**; display threshold $P < 0.001$ uncorrected; cluster size > 100 voxel) and under oxytocin (**B**; display threshold $P < 0.001$ uncorrected; cluster size > 100 voxel). Abbreviations: OXT; oxytocin; PLC, placebo.

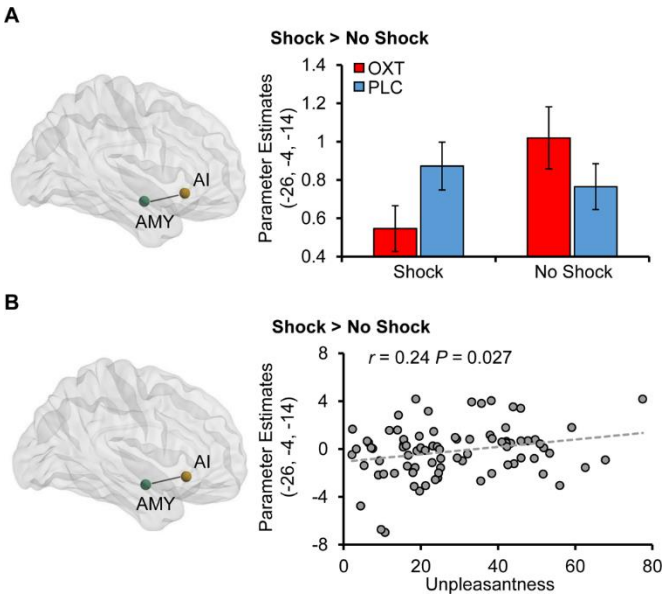

Figure S2. Intranasal oxytocin significantly reduced the functional connectivity from the left anterior insula (AI) as seed region to results the left amygdala (AMY) during the perception of shocks relative to no shocks (**A;** peak MNI coordinates x, y, z: -26, -14, -6; $t_{(240)} = 3.16$, $P_{FWE} < 0.05$, display threshold $P < 0.05$ uncorrected). In the whole sample, a stronger functional coupling of the amygdala and anterior insula correlated with more unpleasant experience of shocks (**B;** $r = 0.24$, $P < 0.05$). Seed regions are color-coded in brown. Error bars indicate the standard error of the mean (SEM). Abbreviations: AI, anterior insula; AMY, amygdala; L, left hemisphere; OXT, oxytocin; PLC, placebo; R, right hemisphere.

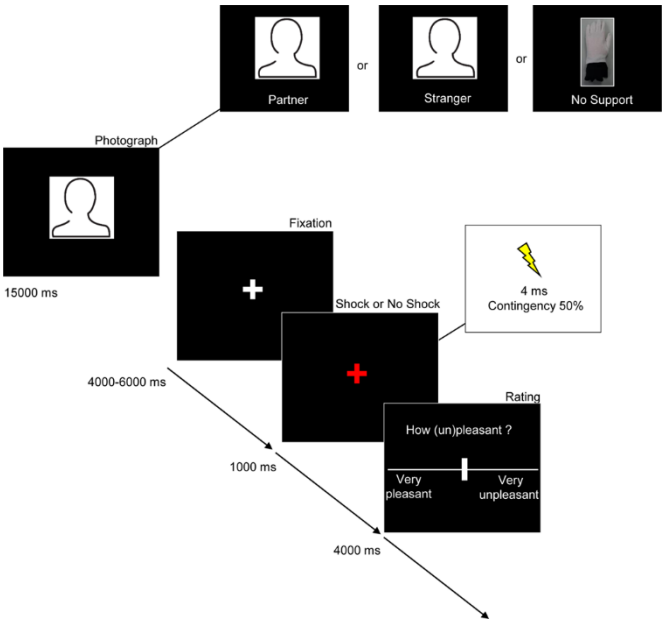

Figure S3. Task design. During the functional magnetic resonance imaging task, participants received social support from their romantic partner, an unfamiliar experimenter or no support while unpleasant electric shocks were delivered to the subject's lower arm.

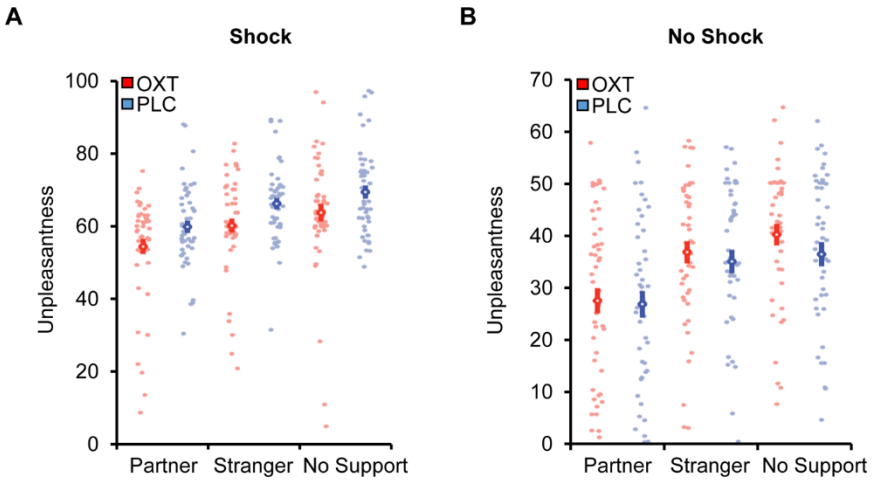

Figure S4. Distribution of the unpleasantness ratings of shocks (**A**) and no shocks trials (**B**) under partner support, stranger support, and no support after the administration of oxytocin (OXT) or placebo (PLC) nasal spray. The unfilled dot represents the mean and the error bars indicate the standard error of the mean (SEM). Abbreviations: OXT, oxytocin; PLC, placebo.

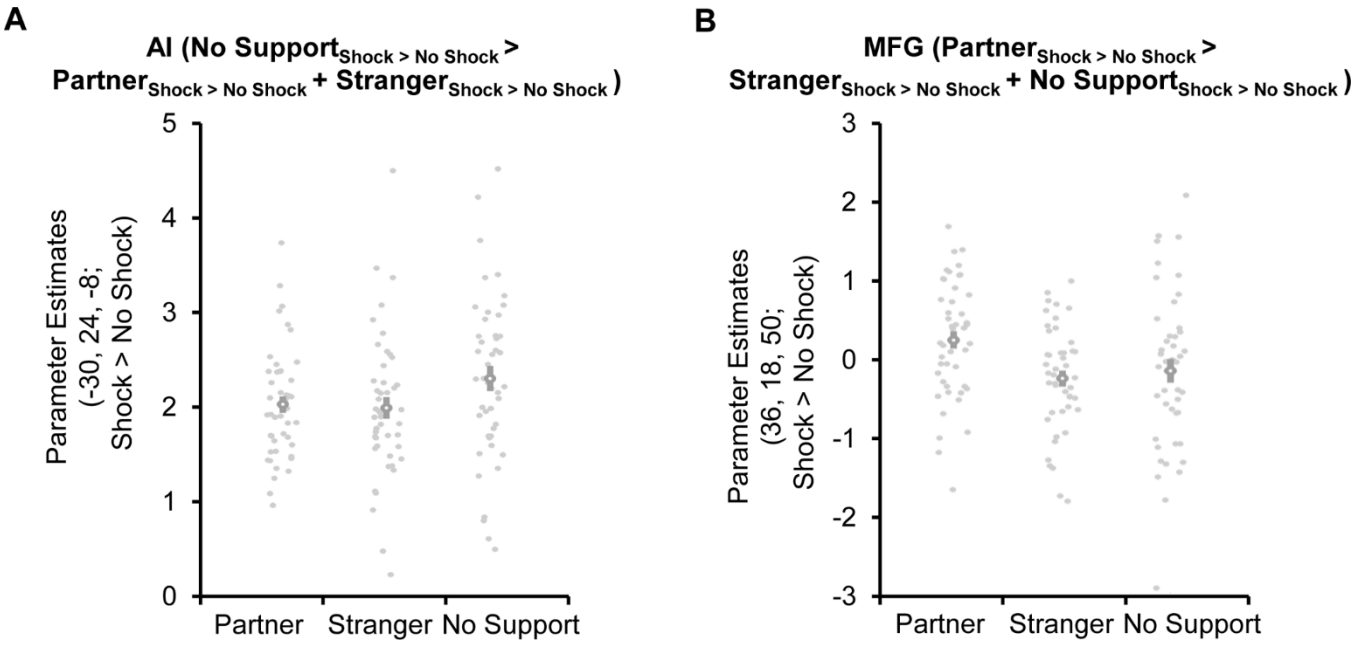

Figure S5. Distribution of the parameter estimates indicating the neural responses to shocks relative to no shocks under partner and stranger support compared to no support in the left anterior insula under placebo (AI; **A**). Distribution of the parameter estimates representing the neural responses to shocks relative to no shocks under partner support compared to stranger and no support in the right middle frontal gyrus after placebo treatment (MFG; **B**). The unfilled dot represents the mean and the error bars indicate the standard error of the mean (SEM). Abbreviations: AI, anterior insula; MFG, middle frontal gyrus.

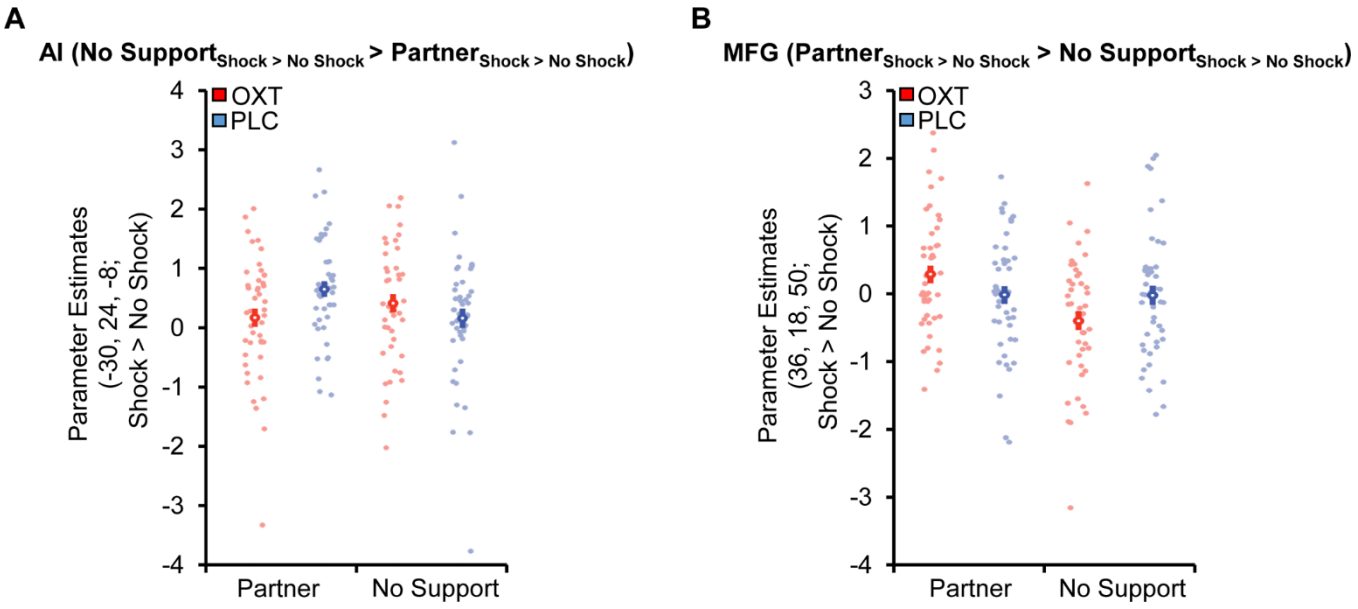

Figure S6. Distribution of the parameter estimates indicating the neural responses to shocks relative to no shocks under partner support compared to no support in the left anterior insula (AI; **A**) and the right middle frontal gyrus (MFG; **B**) under oxytocin (OXT) and placebo (PLC). The unfilled dot represents the mean and the error bars indicate the standard error of the mean (SEM). Abbreviations: AI, anterior insula; MFG, middle frontal gyrus; OXT, oxytocin; PLC, placebo.

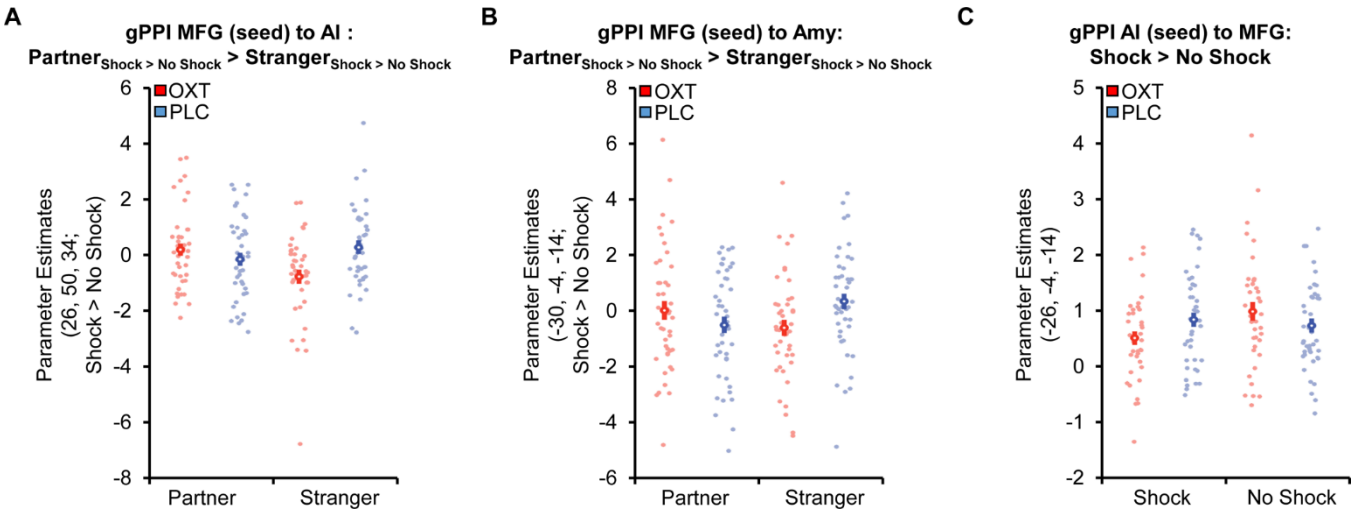

Figure S7.

Distribution of the parameter estimates of the oxytocin (OXT) and placebo (PLC) group representing the functional coupling of the right anterior insula (AI; seed region) to the right middle frontal gyrus (MFG; **A**) and of the right MFG (seed region) to the left amygdala (AMY) during partner support relative to stranger support (**B**). The parameter estimates under OXT and PLC indicating the functional coupling of the left AI (seed region) to the left AMY during the processing of shocks relative to no shocks (**C**). The unfilled dot represents the mean and the error bars indicate the standard error of the mean (SEM). Abbreviations: AI, anterior insula; AMY, amygdala; MFG, middle frontal gyrus; OXT, oxytocin; PLC, placebo.

References

Baron-Cohen, S., Wheelwright, S., Skinner, R., Martin, J., & Clubley, E. (2001). The autism-spectrum quotient (AQ). evidence from Asperger syndrome/high-functioning autism, males and females, scientists and mathematicians. *Journal of autism and developmental disorders, 31*, 5-17.

Bierhoff H. W., Grau, I., & Ludwig A. (1993). Marburger Einstellungs-Inventar für Liebesstile (MEIL) [Marburg attitude inventory of love styles]. Goettingen: Hogrefe.

Hautzinger, M., Bailer, M., Worall, H., & Keller F. (1995). Beck-Depressions-Inventar (BDI). Bern: Huber.

Kreuder, A.K., Scheele, D., Wassermann, L., Wollseifer, M., Stoffel-Wagner, B., Lee, M.R., Hennig, J., Maier, W., & Hurlemann, R. (2017). How the brain codes intimacy: The neurobiological substrates of romantic touch. *Human Brain Mapping, 38,* 4525-4534.

Mattick, R.P., & Clarke, J.C. (1998). Development and validation of measures of social phobia scrutiny fear and social interaction anxiety. *Behaviour Research and Therapy, 36*, 455-470.

McLaren, D.G., Ries, M.L., Xu, G., & Johnson, S.C. (2012). A generalized form of context-dependent psychophysiological interactions (gPPI): a comparison to standard approaches. *NeuroImage*, *61*, 1277-1286.

Spielberger, C.D., Gorsuch, R.L., & Lushene, R.E. (1970). Manual for the State-Trait Anxiety Inventory. Palo Alto, CA: Consulting Psychologists Press.

Stangier, U., Heidenreich, T., Berardi, A., Golbs, U., & Hoyer, J. (1999). Die Erfassung sozialer Phobie durch die Social Interaction Anxiety Scale (SIAS) und die Social Phobia Scale (SPS). [Assessment of social phobia by the Social Interaction Anxiety Scale (SIAS) and the Social Phobia Scale (SPS)] *Zeitschrift für Klinische Psychologie, 28*.

Watson, D., Clark, L.A., & Tellegen, A. (1998). Development and validation of brief measures of positive and negative affect: the PANAS scales. *Journal of Personality and Social Psychology, 54,* 1063-1070.

Xia, M., Wang, J., & He, Y. (2013). BrainNet Viewer: a network visualization tool for human brain connectomics. *PloS one, 8*, e68910.